第 43 卷 第 16 期/2023 年 8 月/光学学报 封底文章·特邀综述

光学学报

基于矢量光场的等离激元模式调控

肖发俊[1,2*]，赵建林[1,2**]

[1]西北工业大学物理科学与技术学院，陕西 西安 710129；

[2]西北工业大学光场调控与信息感知工业和信息化部重点实验室，陕西 西安 710129

摘要 表面等离激元因其极强的束缚光场能力，成为亚波长尺度下研究光与物质相互作用的理想平台，也是构建未来小型化、低功耗、高便携光电子器件的核心单元。更多维度、更加精确和灵活地调控等离激元的模式性质对推动其基础和应用研究至关重要。近年来，光场调控技术的发展，拓展了人们利用光场的维度，也赋予光场更强大的操控等离激元模式的能力。本文简述了矢量光场与等离激元模式作用的基本理论与物理机制，回顾了近年来矢量光场调控等离激元模式激发、耦合和远场辐射的研究进展，并介绍了相关研究在增强光谱、纳米颗粒光捕获、纳米位移传感等方面的应用。

关键词 表面等离激元；矢量光场；模式耦合；单向散射

中图分类号 O436 **文献标志码** A **DOI**：10.3788/AOS230854

1 引 言

随着通信数据量的激增和设备便携性要求的增长，光电子器件的高集成度、超小型化与低功耗已成为其发展的必然趋势。等离激元可以突破衍射极限，将光波的能量限域在亚波长尺度内，是微纳尺度下光子操纵与集成的优良载体，因此成为构建未来光电子器件的理想选择[1-3]。近年来，等离激元的研究拓展了人们对光与物质相互作用的认识，也极大促进了太阳能电池[4]、生物医学检测[5]、光催化[6]、新型光源[7]、信息存储[8]、处理及显示[9]等应用领域的发展，成为纳米光子学最为活跃的研究方向之一。

等离激元的相关应用离不开对其共振模式性质的探究。通过探索强局域等离激元模式的高效产生方法，进而选择模式的类型与相位差，能操控模式叠加来裁剪近场分布，并能借助模式间的干涉，调节结构远场的分布。以此，可实现灵活可控的近场和远场，从而为多种功能化应用提供亚波长平台。例如，激发等离激元的高阶模式可生成强局域电磁场，为稳定捕获亚波长颗粒甚至单分子操控提供了有效的途径[10]。调谐等离激元亮模式和暗模式的耦合，能够产生Fano共振现象，通过其非对称、尖锐的光谱线型可实现高灵敏度的生物化学传感[11]。借助等离激元模式的耦合，还可以有效地调控远场辐射[12]或片上光传输的特性[13]，实现局域能量与远场能量的高效转化，以此可提升纳米光源的方向性[14]。等离激元灵活的可调性，也为上述模式操控提供了可能。典型地，形貌、尺寸、间隙等几何构型的变化会带来等离激元边界条件的改变，进而实现模式响应的显著调谐[15]。除了静态调控外，利用相变[16]、液晶[17]等材料带来的环境折射率的改变也可以实现等离激元模式的动态控制。更引人注目的是，光场调控技术的飞速发展，大大提升了光场利用的自由度，为调控光与物质的相互作用提供了丰富、灵活的手段[18]。例如，通过对光场振幅、相位、偏振等的调制，已发展出多种超分辨成像技术[19]；通过对光场的时域调控，可实现分子转动、解离、电离等过程的精密控制[20]；通过对光场的相干性和偏振态的调控，可提高非线性光学过程的转换效率[21-22]。相应地，这些调控方法也被陆续应用于等离激元的研究中，为拓展和开发等离激元的相关应用开辟了全新的途径。本文将讨论矢量光场对等离激元模式激发、耦合和辐射过程的调控，并介绍相关的基本原理、现象与应用。

2 等离激元模式的激发

2.1 紧聚焦矢量光场与等离激元结构的作用

相较于传统的标量光场，矢量光场可通过紧聚焦及焦场调控的方法，生成亚波长尺度的高度局域且任意设计的光场偏振分布。这为提高光场与亚波长等离激元结构的耦合效率，特别是激发高阶的等离激元模式提供了便利。以柱矢量光场为例，通过高数值孔径

收稿日期：2023-04-21；**修回日期**：2023-06-08；**录用日期**：2023-06-26；**网络首发日期**：2023-07-13

基金项目：国家重点研发计划(2022YFA1404800)、国家自然科学基金(12274345,11634010,11874050)、陕西省自然科学基础研究计划(2021KW-19)、中央高校基本科研业务费(D5000210936,3102019JC008)

通信作者：*fjxiao@nwpu.edu.cn；**jlzhao@nwpu.edu.cn

($NA>0.7$)物镜的聚焦后，焦场的电矢量分布可由理查德-沃尔夫矢量衍射理论计算获得。如入射光场为径向矢量光，则焦场的径向分量E_ρ和纵向分量E_z[23]分别为

$$\begin{cases} E_\rho(\rho,z)=A\int_0^\alpha \cos^{1/2}\theta\sin(2\theta)l_0(\theta)\mathrm{J}_1(k\rho\sin\theta)\mathrm{e}^{\mathrm{i}kz\cos\theta}\mathrm{d}\theta \\ E_z(\rho,z)=2\mathrm{i}A\int_0^\alpha \cos^{1/2}\theta\sin^2\theta l_0(\theta)\mathrm{J}_0(k\rho\sin\theta)\mathrm{e}^{\mathrm{i}kz\cos\theta}\mathrm{d}\theta \end{cases}, \tag{1}$$

式中：A为常数；α为物镜的最大会聚角；l_0为入射光场的振幅；$\mathrm{J}_n(k\rho\sin\theta)$为$n$阶第一类贝塞尔函数。若入射光场为角向矢量光，则焦场只有角向分量E_ϕ[23]可表示为

$$E_\phi(\rho,z)=2A\int_0^\alpha \cos^{1/2}\theta\sin\theta l_0(\theta)\mathrm{J}_1(k\rho\sin\theta)\mathrm{e}^{\mathrm{i}kz\cos\theta}\mathrm{d}\theta。 \tag{2}$$

基于上述光场聚焦的矢量衍射理论，可数值计算得到径向和角向矢量光束在紧聚焦条件下($NA=0.9$)焦场的电场强度、偏振和相位分布，如图1所示。可以看出，聚焦的径向矢量光束，除了呈环形强度分布的径向电场分量外，还会在光轴附近产生亚波长尺度的纵向电场分量，且纵向分量强于横向分量[23]；聚焦的角向矢量光束，则只有角向的电场分量，总电场呈中空的强度分布，与聚焦前的电场分布相同。聚焦的矢量光场与等离激元结构的作用可以用本征响应理论描述[24-27]。据此，在入射光场$\boldsymbol{E}_{\mathrm{inc}}$的作用下，结构的电极化强度$|P\rangle$可看成各阶共振模式$\boldsymbol{P}_j$的叠加[27]，则

$$|P\rangle=\sum_j \alpha_{\mathrm{eig},j}|P_j\rangle\langle P_j|E_{\mathrm{inc}}\rangle, \tag{3}$$

式中：$\alpha_{\mathrm{eig},j}=\lambda_j^{-1}$为模式$j$的本征极化率；$\langle P_j|E_{\mathrm{inc}}\rangle$表示共振模式$|P_j\rangle$相对于入射电场$E_{\mathrm{inc}}$的投影强度。等离激元结构的辐射强度[26]可表示为

$$|k|P\rangle=\sum_j \alpha_{\mathrm{eig},j}|k|P_j\rangle\langle P_j|E_{\mathrm{inc}}\rangle, \tag{4}$$

式中，$|k\rangle$代表辐射平面光波波矢$\boldsymbol{k}$。可以看出，结构的辐射强度可由$\langle P_j|E_{\mathrm{inc}}\rangle$所决定。由此，通过调控矢量光聚焦场的偏振态分布来匹配模式的极化强度，即可

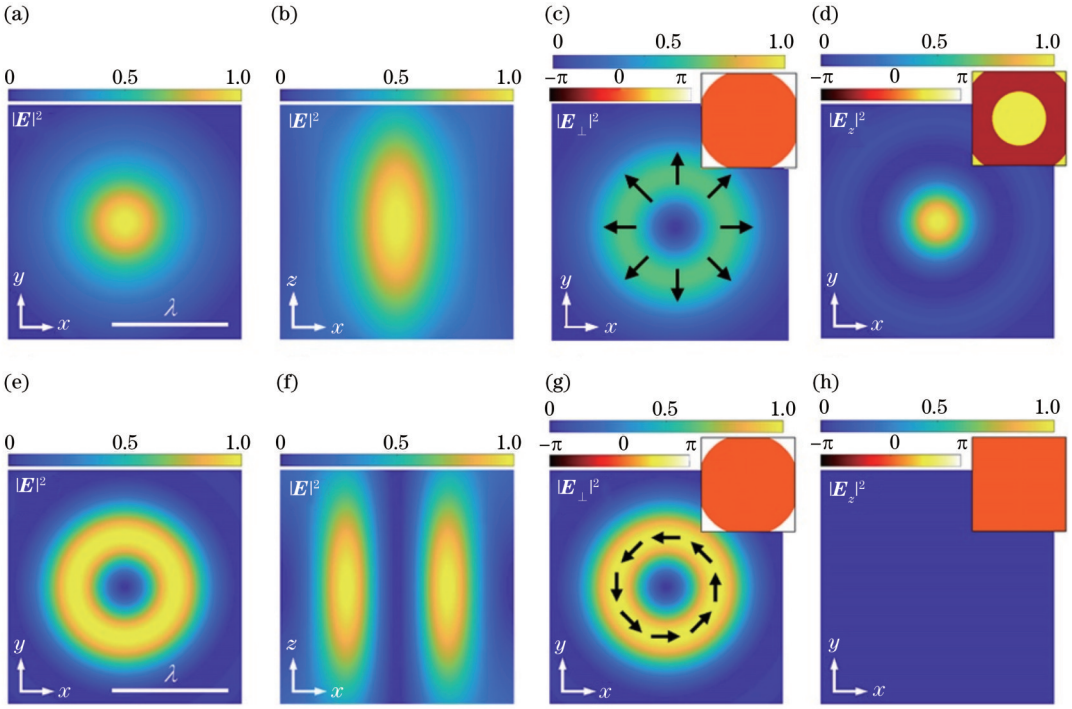

图1　紧聚焦条件($n=1$，$NA=0.9$，$\beta_0=1$)下，矢量光束焦场的电场强度、偏振和相位分布。(a)～(d)径向偏振矢量光束；(e)～(h)角向偏振矢量光束。(a)、(e)总电场强度($|\boldsymbol{E}|^2=|\boldsymbol{E}_x|^2+|\boldsymbol{E}_y|^2+|\boldsymbol{E}_z|^2$)在$xy$平面的分布；(b)、(f)总电场强度在$xz$平面的分布；(c)、(g)横向电场强度($|\boldsymbol{E}_\perp|^2=|\boldsymbol{E}_x|^2+|\boldsymbol{E}_y|^2$)；(d)、(h)纵向电场强度($|\boldsymbol{E}_z|^2$)。图中黑色箭头代表偏振态，插图表示相位分布

Fig. 1　Electric field intensity, polarization, and phase distributions of tightly focused cylindrical vector beams ($n=1$, $NA=0.9$, $\beta_0=1$). (a)-(d) Radially polarized vector beam; (e)-(h) azimuthally polarized vector beam. (a), (e) Distribution of total electric field intensity ($|\boldsymbol{E}|^2=|\boldsymbol{E}_x|^2+|\boldsymbol{E}_y|^2+|\boldsymbol{E}_z|^2$) in xy plane; (b), (f) distribution of total electric field intensity in xz plane; (c), (g) transverse electric field intensity ($|\boldsymbol{E}_\perp|^2=|\boldsymbol{E}_x|^2+|\boldsymbol{E}_y|^2$); (d), (h) longitudinal electric field intensity ($|\boldsymbol{E}_z|^2$). The dark arrows represent polarization states and insets are for phase distributions

高效激发特定模式。特别地，借助高阶柱矢量光、杂化偏振矢量光等，可在结构中激发多个模式，并能调整不同模式的权重，以此实现等离激元近场分布[28-29]、传输[13]以及辐射远场分布及光谱线型的调节[30]。

2.2　矢量光场对等离激元模式激发的调控

电偶模式是等离激元结构中最常见的一类模式。它具有强的远场辐射能力和较宽的共振峰，也被称为“亮模式”，可方便地通过光学的方式来激发[31]。例如，具有面内偶极矩的电偶模式可以由常用的线偏光来激发。然而，纵向的电偶模式因在衬底法线方向上的辐射能力较弱，则很难由聚焦的线偏光激发，为其观测和应用带来了困难[32]。紧聚焦的径向矢量光场在焦点处有很强的电场纵向分量，借助焦场与电偶极矩的匹配，则能高效激发纵向等离激元电偶模式。如图 2(a)所示，Krasavin 等[33]借助紧聚焦的径向矢量光束，在金纳米小球中激发出纵向的电偶极共振模式。需要注意的是，对于紧聚焦的径向矢量光场，焦平面上面内和纵向电场的叠加会生成三维分布的电矢量[34][图 2(b)上图]。由此，通过移动金纳米球在焦场中的位置，利用电矢量匹配调控偶极矩方向，则能实现任意方向电偶模式的激发[35]，如图 2(b)下图所示。这种灵活调控的电偶极矩可应用于等离激元-分子相互作用的研究中，借助电偶极矩与分子的跃迁偶极矩相对夹角的调节，可改变等离激元-分子的耦合强度，有望推动单分子级的物性表征及高分辨率的远场偏振显微镜的研发。除了电偶模式的匹配激发外，借助聚焦的角向矢量光场，还能生成强纵向磁分量的焦场，可以匹配激发等离激元的磁偶模式，并实现 5 个数量级的局域场强度增强[36]，如图 2(c)所示。

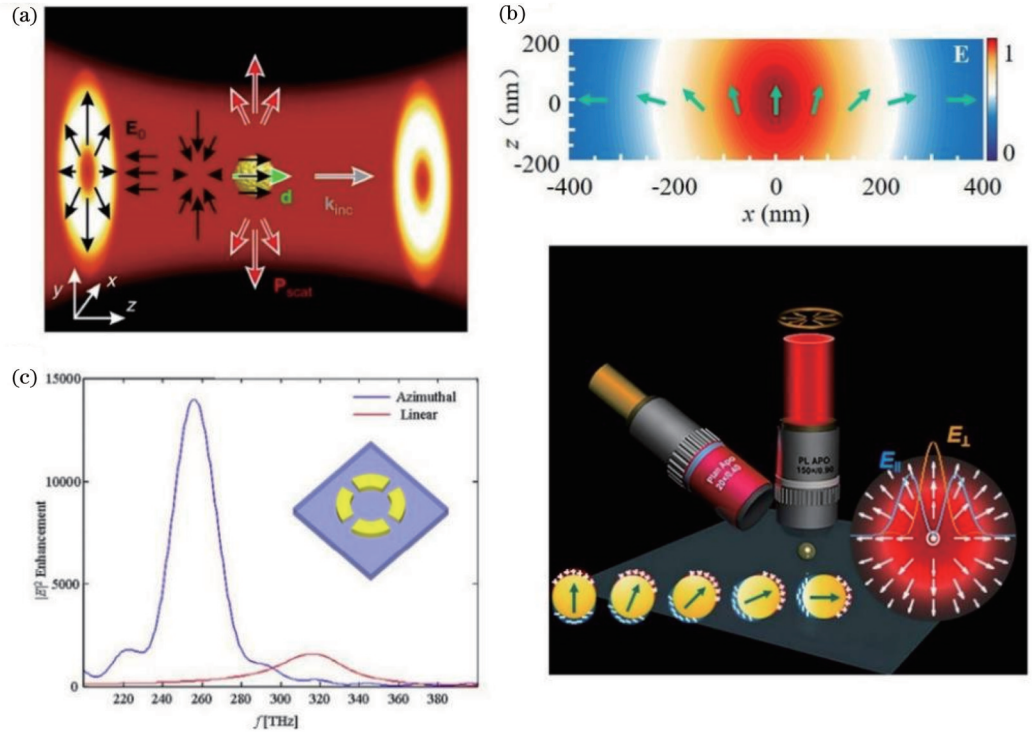

图 2　矢量光场对等离激元偶极模式的激发与调控。(a)紧聚焦径向偏振矢量光对金纳米球中纵向偶级模式的激发[33]；(b)径向矢量光焦场的电矢量分布(上图)，及其激发的任意方向的电偶极矩(下图)[35]；(c)角向偏振矢量光束激发的磁偶模式[36]

Fig. 2　Excitation and manipulation of plasmonic dipole modes with vector beam. (a) Longitudinal electrical dipole in an Au nanosphere excited by tightly focused radially polarized vector beam[33]; (b) electric vector distribution of radial vector focal field (upper panel) and electric dipole distance in any direction excited by it (below panel) [35]; (c) magnetic dipole mode excited by azimuthally polarized vector beam[36]

除亮模式外，等离激元结构还支持一类偶极矩为零的模式，即暗模式[37]。该类模式具有较小的辐射损耗、较窄的共振峰和更为显著的局域场增强效应。这些性质使暗模式在增强光与物质的相互作用方面，表现出无与伦比的优势。目前，暗模式已广泛用于表面增强拉曼散射[38]、增强非线性光学效应[39]、生物传感[40]，以及纳米激光[41]等研究中。然而，暗模式由于极小的净偶极距，很难直接被常规的标量光场激发，需借助聚焦的高速电子[42](如电子能量损失能谱法和阴极发光技术)或倏逝场来实现观测[43]。这些较为复杂的激发方式对暗模式的实际应用带来了困难。相比之下，矢量光场可以与普通光学显微镜兼容，利用其焦场丰富的偏振态分布，可以方便灵活地激发、观测等离激元暗模式。以电四模式为例，它可以看成两个反相电

偶模式的集合，故总的净偶极矩为零，是最常见的一类暗模式。图 3(a)给出了利用聚焦径向矢量光激发电四模式的结果[44]。可以看出，当金纳米棒与径向矢量光束同轴时(y=0)，具有柱对称分布的径向电场分量与镜面对称的长轴偶数阶共振模式完全匹配[如图 3(a)左图所示]，所以投影强度$\langle P_{l=2}|E_{\mathrm{inc}}\rangle \neq 0$，可高效地激发电四模式。同样，基于模式极矩匹配的方法，还可在等离激元多聚体结构中激发出更为复杂的暗模式。2014 年，Yanai 等[45]利用聚焦的径向和角向矢量光束分别激发了金纳米盘七聚体的径向和角向暗模式，如图 3(b)所示。此外，Bao 等[46]还设计了一种金膜-介质层-六聚体等离激元结构[如图 3(c)左图所示]。通过在照明光中引入径向矢量光，可以匹配结构中的环偶极子模式，并在散射光谱中观察到了该模式的共振峰[如图 3(c)右图所示]。由于径向激发光的引入，该方案大大简化了传统环偶超材料的结构复杂性。

以矢量光场为激发光，为观测、表征等离激元模式提供了便利，也推进了等离激元的相关应用，如增强光谱、纳米粒子捕获、增强非线性光学效应等。2006 年，Anger 等[47]采用紧聚焦的径向矢量光束作照明光，选择性激发了金纳米球的等离激元模式并使之与荧光分子垂直偶极子相互作用，结果如图 4(a)所示。他们发现，荧光强度会随分子-纳米球间距减小，出现先增大后减小的规律，并进一步揭示了荧光增强中局域场增强和荧光猝灭效应的竞争机制。再者，利用角向矢量光，Zhang 等[48]在等离激元环形团簇针尖上激发了角向模式，并在团簇间隙处形成了强的局域电场。相较于线偏光激发的模式，该角向模式使表面增强拉曼探测灵敏度获得了 2 个数量级的提升，如图 4(b)所示。

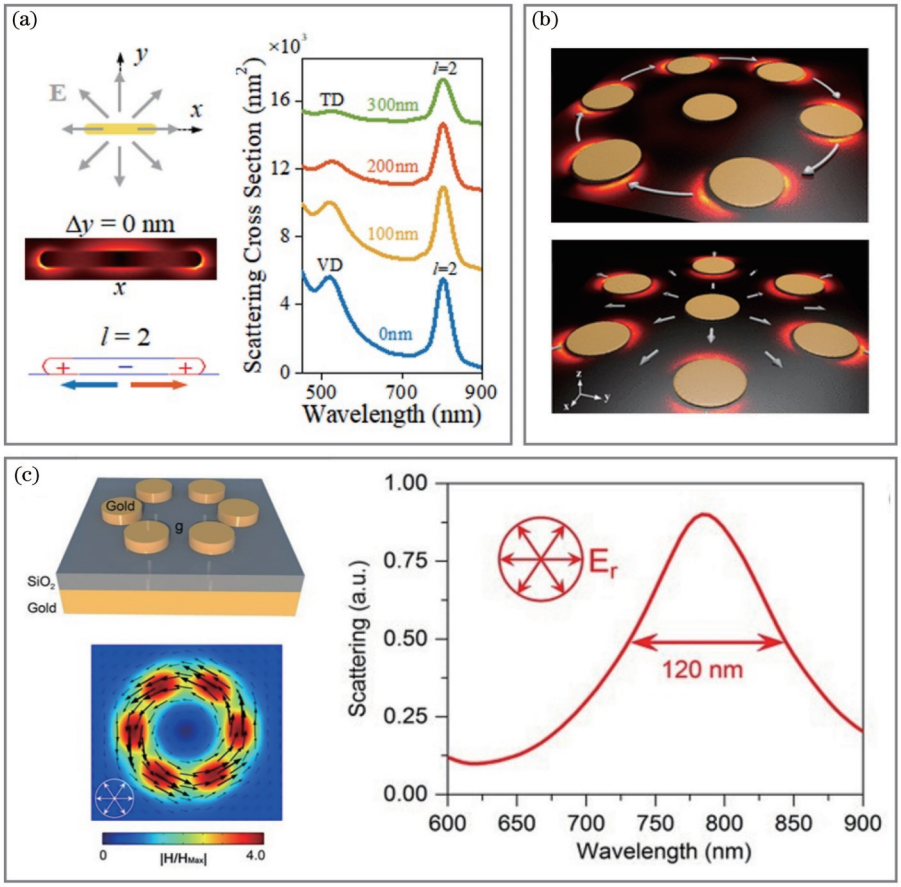

图 3　矢量光场对等离激元暗模式的激发。(a) 紧聚焦径向偏振矢量光在金纳米棒中激发的电四模式[44]。其中，左图为相对于纳米棒的激发光配置，右图为纳米棒在不同y轴位移下的散射光谱；(b) 矢量光在金纳米盘七聚体中选择性激发的径向和角向暗模式[45]；(c) 径向偏振矢量光在金膜-介质层-六聚体中激发的环偶极子[46]。其中，左图为等离激元结构的示意图和激发矢量光的磁场分布，右图为环偶极子的散射光谱

Fig. 3　Excitation of plasmonic dark modes with vector beam. (a) Electric quadrupole mode of Au nanorod generated by a tightly focused radially polarized vector beam[44]. Left and right panels are for excitation configuration relative to nanorod and scattering spectra of nanorod at different y displacements, respectively; (b) selectively exciting azimuthal and radial plasmonic dark modes by vector beam in Au nanodisk heptamers [45]; (c) toroidal dipole mode excited in gold film-dielectric layer-hexamer using radially polarized vector beam[46]. Left and right panels are schematics of plasmonic structure as well as magnetic field distributions of vector beam and scattering spectrum of toroidal dipole mode, respectively

借助矢量光束激发的强局域等离激元暗模式，能产生较大的近场增强和梯度，在较低光功率下即可实现纳米颗粒的稳定捕获。例如，图 4(c)表明，聚焦的径向矢量光可在等离激元环形光阑激发出径向呼吸模式。由于该暗模式可将近场束缚在纳米宽度的环形光阑内，由此产生了陡峭的捕获光阱，从而在毫瓦量级光功率下实现了 5 nm 电介质小球的稳定捕获[49]。另外，径向矢量光还能够在镀金属膜光纤锥-金衬底组成的等离激元纳米腔中激发出间隙暗模式。借此，在纳腔中生成 10 nm 尺度的“热点”，可完成 2 nm 半导体量子点的稳定捕获[图 4(d)]，为单颗粒级的光学捕获与原位物性表征提供了一种方案[50]。在光学非线性方面，借助矢量激发场对等离激元模式进行选择性的激发，还可以改变增强二次谐波的输出频率。例如，通过切换激发光由高斯线偏振光至径向矢量光再至角向矢量光，可分别匹配激发八聚体纳米盘的反键电偶模式、径向和角向模式，以此借助基频光共振波长的改变实现倍频光频率的调节[51]，结果如图 4(e)所示。这种简单

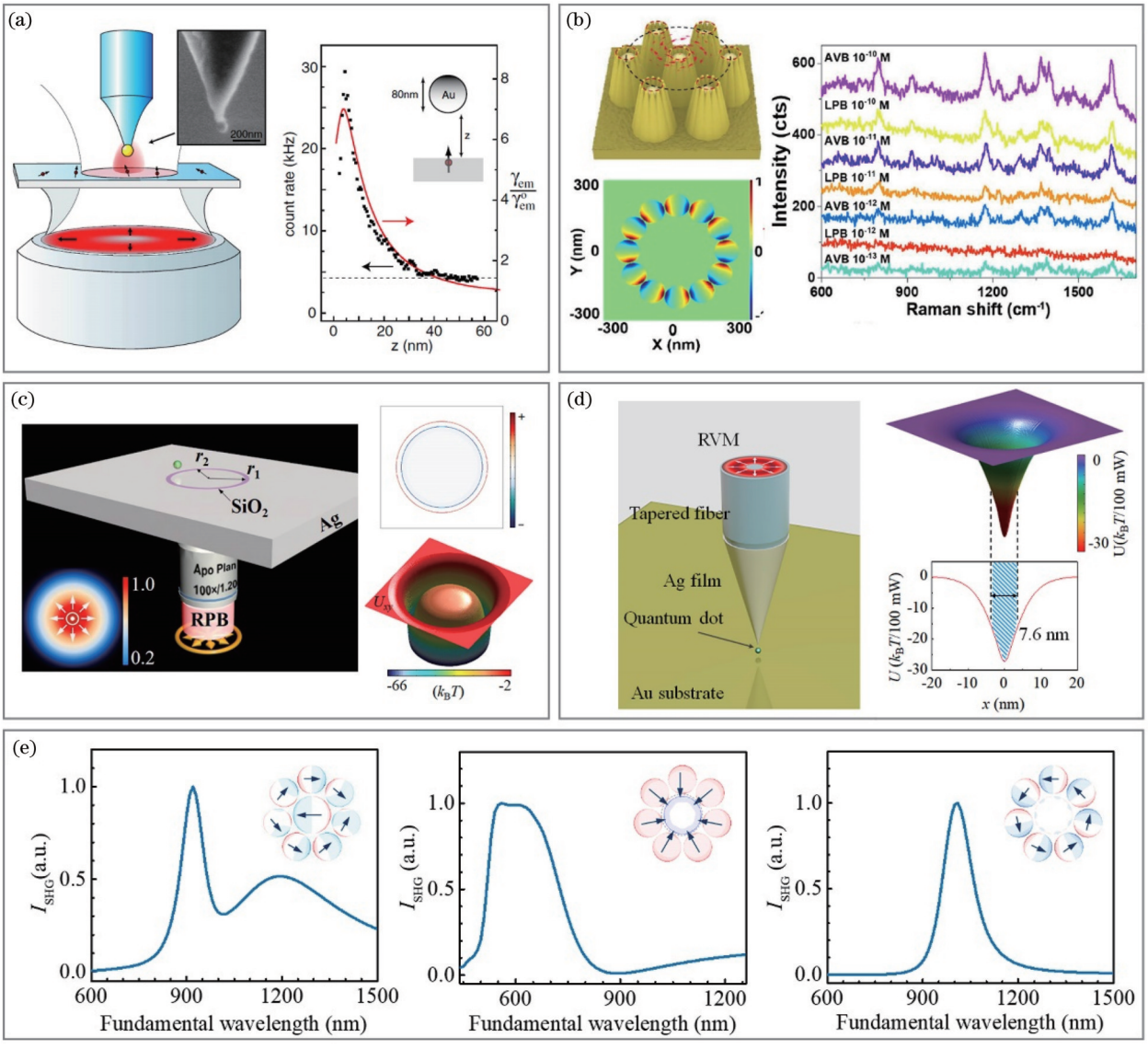

图 4　等离激元模式的高效光激发与应用。(a)紧聚焦的径向偏振矢量激发光对等离激元电偶模式-荧光分子相互作用的控制[47]；(b)角向等离激元暗模式的激发及在表面增强拉曼光谱中的应用[48]；(c)银纳米光阑中的径向呼吸模式及其对 5 nm 介质纳米球的光学捕获[49]；(d)径向矢量光激发的等离激元纳米腔模式对 2 nm 量子点的光学捕获[50]；(e)基于矢量光场的模式匹配实现八聚体纳米盘二次谐波频率的调谐[51]

Fig. 4　Efficient excitation and applications of plasmonic modes. (a) Manipulation of interaction between plasmonic dipole mode and fluorescence molecule using tightly focused radially polarized vector beam[47]; (b) excitation of azimuthal plasmonic dark mode and its applications in surface enhanced Raman spectroscopy[48]; (c) radial breathing mode in silver nanoaperture and its optical trapping of 5 nm dieletric nanosphere[49]; (d) optical trapping of 2 nm quantum dot[50] using plasmonic cavity mode excited by radial plasmonic breathing mode; (e) tuning frequency of second harmonic generation from octamer nanodisk using mode matching technique based on vector beam[51]

易行的光调控方法为可调谐的非线性相干源开辟了新的途径。

3　等离激元模式耦合的调控

3.1　等离激元模式的耦合模型

根据 Huckel 分子轨道杂化概念，Prodan 等[52]提出了表面等离激元杂化理论，可直观地描述模式间的强耦合行为。根据等离激元杂化理论，自由电子可以看作均匀分布在正电荷背景上不可压缩的无旋流。若该电子流发生形变，便会在金属表面引起表面电荷密度分布，而表面等离激元可以认为是电子流的自激振荡。通过计算整个系统的拉格朗日量，可确定电子流微小形变的动力学方程，进而得到系统的等离激元共振模式。以金属球壳为例，它可以看作金属纳米球形腔和纳米球的组合[52]，如图 5 所示。假设金属的介电常数由 Drude 模型给出，即 $\varepsilon(\omega)=1-\omega_{\mathrm{B}}^2/\omega^2$，其中 $\omega_{\mathrm{B}}=\sqrt{4\pi e^2 n_0/m_{\mathrm{e}}}$ 为金属体材料的等离激元频率（n_0 和 m_{e} 分别为电子的数密度和有效质量）。最终，分别得到金属球形腔和金属球颗粒 l 阶等离激元模式的共振频率[53]为

$$\begin{cases}\omega_{\mathrm{C},l}=\omega_{\mathrm{B}}\sqrt{\dfrac{l+1}{2l+1}}\\ \omega_{\mathrm{S},l}=\omega_{\mathrm{B}}\sqrt{\dfrac{l}{2l+1}}\end{cases}。\tag{5}$$

假设金属球壳的内、外半径分别为 a 和 b，且金属壳层厚度有限。类似于分子轨道的杂化现象，金属球形腔和金属球颗粒各自的等离激元模式会相互耦合，形成金属球壳的等离激元共振模式[52]。根据该杂化理论，可得金属球壳的两个 l 阶等离激元模式的频率[53]为

$$\omega_{l\pm}^2=\frac{\omega_{\mathrm{B}}^2}{2}\left[1\pm\frac{1}{2l+1}\sqrt{1+4l(l+1)x^{2l+1}}\right],\tag{6}$$

式中，$x=a/b$ 为金属球壳内外半径之比。可以看出，金属球壳内外表面的等离激元相互作用，产生了新的杂化等离激元共振模式$|\omega_+\rangle$和$|\omega_-\rangle$。其中，$|\omega_+\rangle$模式为金属球形腔和金属球颗粒间反对称耦合成的反键模式，而$|\omega_-\rangle$模式则为对称耦合的成键模式，如图 5 所示。

另一种处理模式耦合问题的方法是耦合谐振子模型[54]，如图 6 所示。发生耦合的等离激元模式可看成两个弹簧振子，对应的运动方程分别为 $x_{\mathrm{A}}(t)$ 和 $x_{\mathrm{B}}(t)$，其劲度系数分别为 k_{A} 和 k_{B}，模式间的耦合可由劲度系数为 g 的弹簧表示。假如激发光场为矢量光 E，其与两模式的耦合效率分别为 η_{A} 和 η_{B}，则其大小由模式的极化强度$\left|P_j\right\rangle$相对于入射电场 E 的投影强度$\left\langle P_{\mathrm{A,B}}|E\right\rangle$决定。相应地，激发光场会在两个弹簧振子上施加周期性驱动力 $F_{\mathrm{A,B}}$。假设两模式的频率、非辐射损耗和

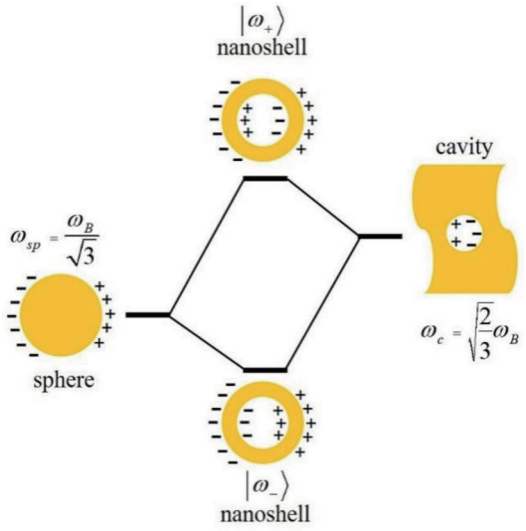

图 5　金属球壳等离激元结构的模式杂化示意图[52]

Fig. 5　Schematic illustration of plasmon hybridization in metallic nanoshell[52]

耦合系数分别为 $\omega_{\mathrm{A,B}}$、$\gamma_{\mathrm{A,B}}$，由此可得耦合模式的动力学方程[54]为

$$\begin{cases}\dfrac{\mathrm{d}^2x_{\mathrm{A}}}{\mathrm{d}t^2}+\gamma_{\mathrm{A}}\dfrac{\mathrm{d}x_{\mathrm{A}}}{\mathrm{d}t}+\omega_{\mathrm{A}}^2x_{\mathrm{A}}+gx_{\mathrm{B}}=\eta_{\mathrm{A}}E\\ \dfrac{\mathrm{d}^2x_{\mathrm{B}}}{\mathrm{d}t^2}+\gamma_{\mathrm{B}}\dfrac{\mathrm{d}x_{\mathrm{B}}}{\mathrm{d}t}+\omega_{\mathrm{B}}^2x_{\mathrm{B}}+gx_{\mathrm{A}}=\eta_{\mathrm{B}}E\end{cases}。\tag{7}$$

这样，等离激元结构的散射光谱可表示为

$$\alpha_{\mathrm{sca}}\propto\left|x_{\mathrm{A}}(\omega)+x_{\mathrm{B}}(\omega)\right|^2。\tag{8}$$

以此，通过式(8)可拟合实验或数值模拟的散射光谱，以提取模式耦合强度等关键物理量。

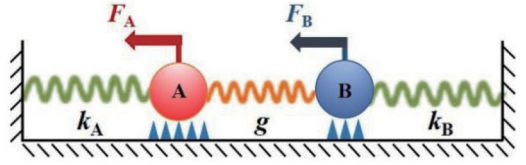

图 6　描述等离激元模式耦合的耦合谐振子模型

Fig. 6　Coupled harmonic oscillator model describing plasmonic mode coupling

3.2　矢量光场对等离激元模式耦合的调控

借助矢量激发场空间依赖的偏振分布，通过极矩匹配的方法可以确定性地选取参与耦合的等离激元模式的相位或类型，从而实现模式耦合的控制。例如，Deng 等[55]分别利用角向和径向矢量光束在相邻金纳米球中激励了反相的电偶模式，由此生成了“肩并肩”和“首尾”耦合的两种暗模式，并利用等离激元杂化模型给予解释，如图 7(a)所示。对等离激元模式耦合的调节，还可以用于生成可控的近场分布。2010 年，Volpe 等[56]提出了一种基于光学逆向设计算法来控制等离激元结构近场的方法，结果如图 7(b)所示。其中，图 7(b)左列为五聚体纳米片上三种不同的目标近

场分布。根据逆向设计算法，他们通过调节多级厄米高斯光束的相位和振幅[图 7(b)右列]，合成了这些目标近场分布所对应的激发远场。以此，在纳米片五聚体既定位置上重建了近场[图 7(b)中列]，实现了近场分布的精确管理。等离激元模式耦合的控制，也为裁剪光谱线型提供了新的途径，最典型的如Fano共振现象。在等离激元结构中，线宽(辐射损耗)较大的模式可视为连续态，如亮模式；反之，线宽较窄的模式则可视为离散态，如暗模式。两类模式的耦合会带来两者相位差的跃变。相应地，在相位跃变波段前后，辐射场出现相消和相长干涉，呈现出非对称的Fano光谱线型[11]。传统上，等离激元Fano共振大多借助结构的对称破缺来实现。2012 年，Sancho-Parramon 等[57]则提出了一种无须打破结构对称破缺而激发Fano共振的方法。他们通过角向矢量光场在高对称的金纳米球二聚体中激发出成键电偶模式与电四模式的耦合，并观察到了Fano光谱凹陷[图 7(c)]。2017 年，Bao 等[58]利用角向矢量光束在金开口环六聚体结构中激发了磁模式间的多重Fano共振，观察到小于 50 nm线宽的光谱凹陷，如图 7(d)所示。该结果有望应用于低损耗、高灵敏度的传感研究中。除此之外，矢量光场还可以激发并调控两个等离激元暗模式的耦合。例如，径向矢量光通过偶极矩匹配的方法在两个嵌套的等离激元六聚体中分别激发出径向呼吸暗模式[59]。两暗模式的耦合随结构参数的变化规律可很好地由耦合谐振子模型解释，并可为其他体系如双壁碳纳米管中径向呼吸拉

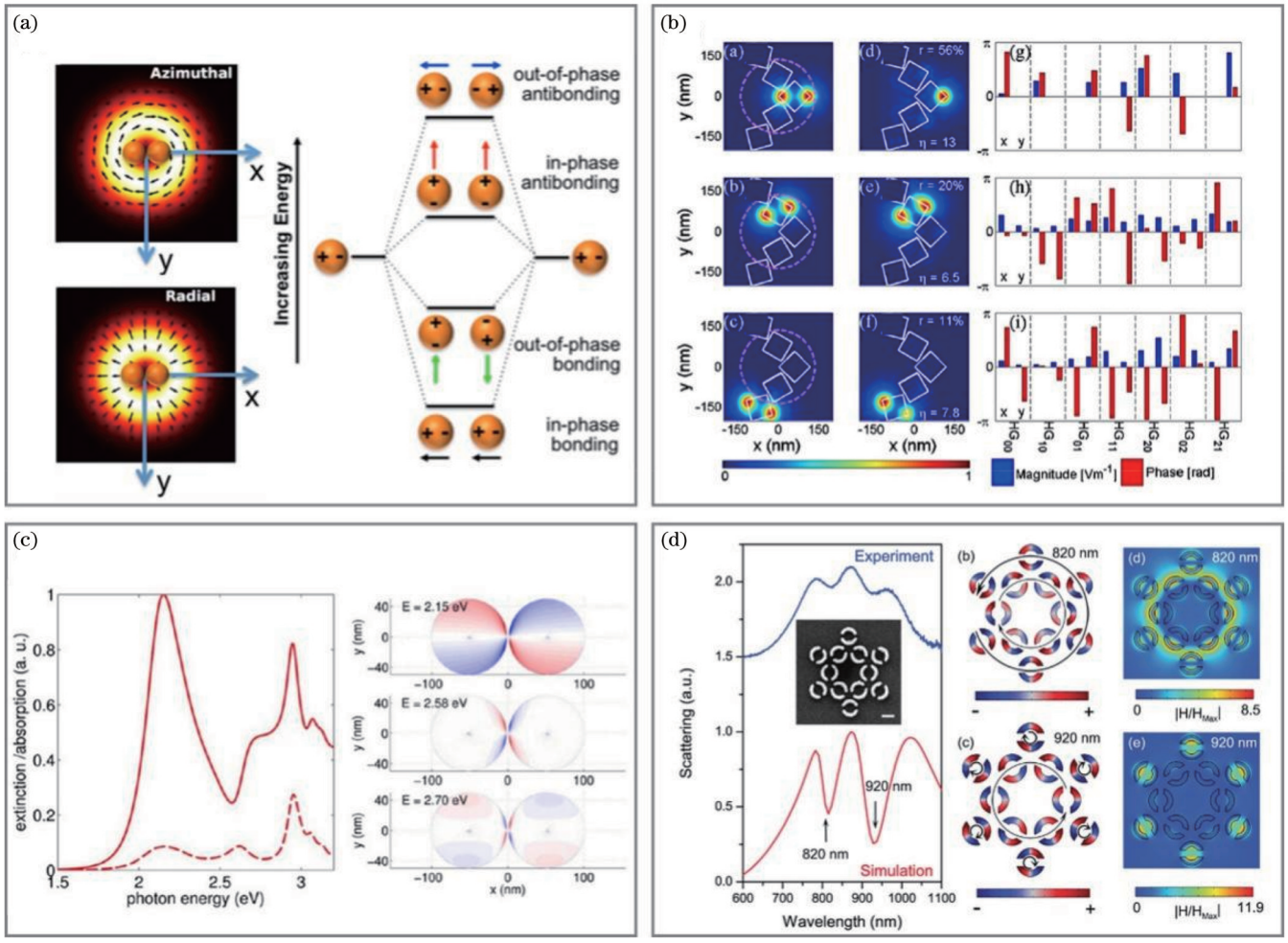

图 7　矢量光场对等离激元模式耦合的控制。(a)角向和径向矢量光在金纳米球二聚体中激发的反相成键和反键的暗模式[55]；(b)厄米-高斯光束对五聚体纳米片近场分布的精确管理[56]，其中，从左到右各列对应目标近场分布、矢量光激发的近场及叠加矢量激发场的各级厄米-高斯光束的振幅与相位；(c)矢量光场在金纳米球二聚体中激发的Fano共振[57]；(d)角向矢量光在开口环多聚体结构中激发的双重Fano共振[58]

Fig. 7　Controlling plasmonic mode coupling with vector beam. (a) Out-of-phase bonding and antibonding dark mode of Au nanosphere dimer excited by azimuthal and radial vector beams[55]; (b) deterministically tuning local field distribution in plasmonic nanocluster using Hermite-Gaussian beams[56], in which left to right panels correspond to target local field, vector beam excited local field as well as amplitudes and phases of Hermit-Gaussian beams for constructing vector excitation; (c) Fano resonance of Au nanosphere dimer under excitation of vector beam[57]; (d) double Fano resonances in a split ring oligomer structure excited by azimuthally polarized vector beam[58]

曼模式的耦合提供借鉴。

矢量光场激发的等离激元模式耦合展现了出众的近场和光谱线型的调控能力，为其在光力控制、二次谐波增强、等离激元结构形貌和缺陷检测中的应用奠定了基础。如图 8(a)所示，在紧聚焦径向偏振矢量光照射时，两纳米银盘的等离激元模式发生强烈杂化，形成成键和反键模式。通过改变二聚体在矢量焦场中的位置等，可以调控杂化类型，导致近场分布在二聚体间隙和外侧的切换，从而实现光结合力方向的翻转，这可为纳米多聚体材料的制备提供新的方法[60]。再如，聚焦的径向矢量光，可调控三聚体纳米盘中径向呼吸暗模式与电偶和电四模式的耦合，进而改变结构的近场分布和光谱线型。通过这种模式耦合调控，可令等离激元模式同时共振增强二次谐波产生的吸收和辐射过程。并且，还可以确保二阶极化强度与倍频处场增强的空间匹配，实现二次谐波的最优输出效率[61]，如图 8(b)所示。另外，图 8(c)显示，可利用角向矢量光在纳米开口环-纳米弧结构中激发 Fano 共振。由于基于光场和纳米结构的空间匹配，该结构的 Fano 线型对光束位置、结构对称性非常敏

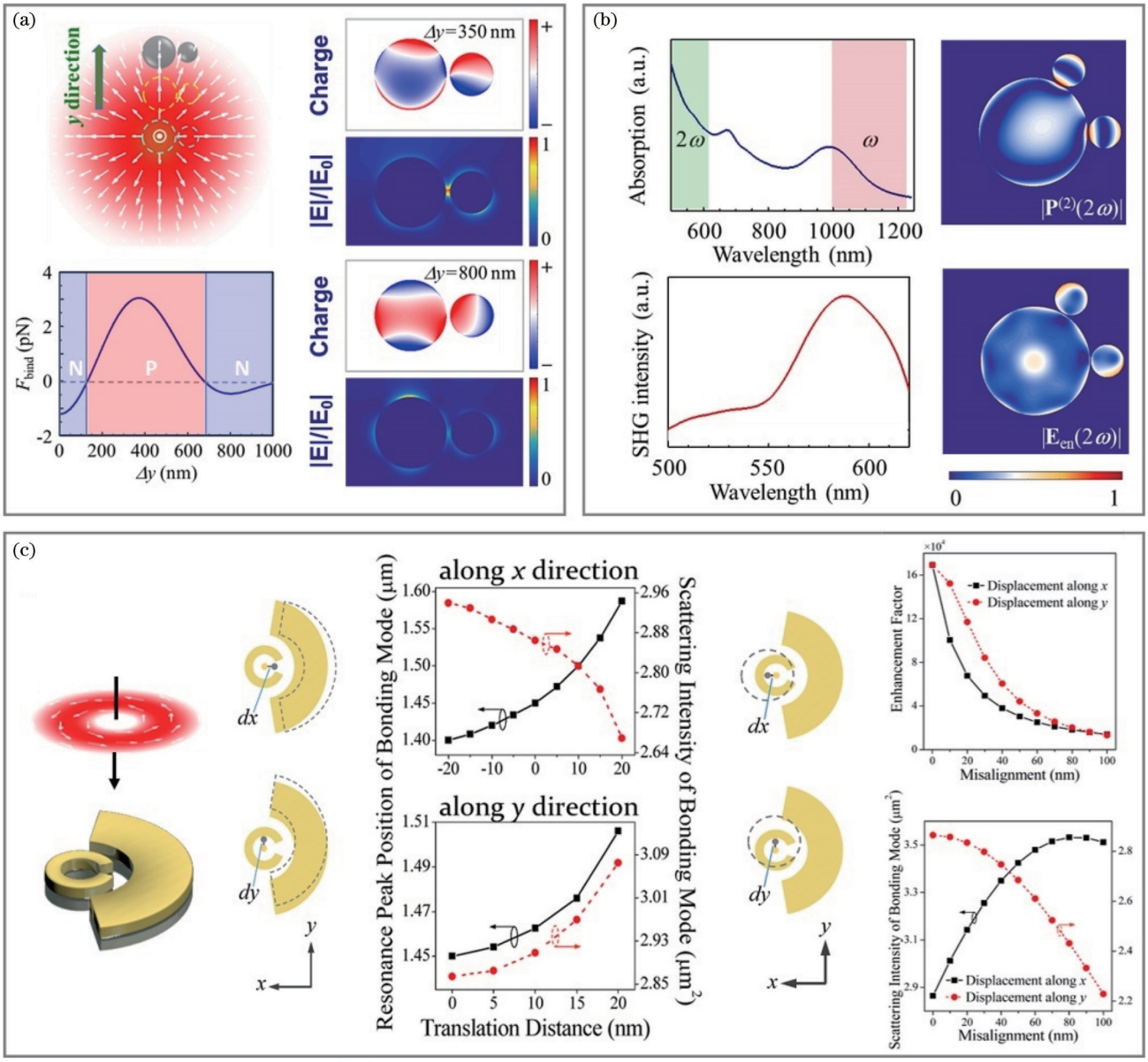

图 8　等离激元模式耦合调控的应用[62]。(a)径向矢量光调控的金纳米盘二聚体间光学结合力的反转；(b)等离子三聚体中基于等离激元模式耦合调控的二次谐波增强；(c)角向矢量光激发的等离激元 Fano 共振在结构缺陷(左图)和光束对准监测(右图)方面的应用

Fig. 8　Applications of vector beam controlled plasmonic mode coupling[62]. (a) Reversible optical binding force in a plasmonic heterodimer by controling mode coupling under illumination of radially polarized vector beam; (b) enhanced second harmonic generation in a plasmonic trimer based on control of plasmonic mode coupling; (c) applications of structural defect (left panel) and beam misalignment (right panel) using plasmonic Fano resonance excited by azimuthally polarized vctor beam

感，故可实现高精度的光束准直和结构加工缺陷的检测[62]。

4　等离激元模式远场辐射分布的调控

4.1　Kerker条件

除了增强近场的光与物质相互作用外，等离激元结构还可以作为光学纳米天线，将局域场的能量或信息，通过辐射转化至远场。同时，借助不同电磁共振模式之间的干涉，实现远场辐射分布的有效调控，最典型的例子如Kerker效应。早在1983年，Kerker预测磁性球颗粒中电偶和磁偶极共振模式的散射电磁场会在远场干涉叠加。并且，当两模式的强度相同，相位差相同或相反时，可在远场实现单一的后向或前向散射，即所谓的Kerker条件[63-64]。随后，更广义的Kerker条件被提出，适用范围也扩展到复杂结构光激发下，多个散射体通过多极模式间的干涉形成任意方向的单向散射。在等离激元研究中，光学八木天线[65]、V形纳米结构[66]、金纳米颗粒二聚体[67]等结构陆续被提出，为单向远场散射的灵活控制提供了便利，也拓展了等离激元在片上信号传输[13]、光学传感[68]、超分辨成像[69]等方面的应用。

现以核壳结构的金属-介质纳米球为例，来考察矢量光场调控的面内散射方向。根据Mie散射理论，面内的左、右向散射强度[70]分别为

$$\begin{cases}\sigma_{\mathrm{d,l}}=\dfrac{9}{4k^2I_{\mathrm{total}}}\left|a_1E_y-b_1ZH_z\right|^2\\ \sigma_{\mathrm{d,r}}=\dfrac{9}{4k^2I_{\mathrm{total}}}\left|a_1E_y+b_1ZH_z\right|^2\end{cases},\tag{9}$$

式中：I_{total}为总电磁场强度；$Z=\sqrt{\mu/\varepsilon}$为背景介质的阻抗，其中μ和ε分别为背景介质的磁导率和介电常数。可以看出，若核壳纳米球的米散射系数a_1和b_1的振幅和相位满足如下条件：

$$\begin{cases}\dfrac{|E_y|}{|ZH_z|}=\dfrac{|b_1|}{|a_1|}\\ \phi_{E_y}-\phi_{ZH_z}=\phi_{b_1}-\phi_{a_1}\end{cases},\tag{10}$$

则$\sigma_{\mathrm{d,l}}=0$，于是便可实现右向单向散射。类似地，实现左向单向散射的条件为

$$\begin{cases}\dfrac{|E_y|}{|ZH_z|}=\dfrac{|b_1|}{|a_1|}\\ \left(\phi_{E_y}-\phi_{ZH_z}\right)-\left(\phi_{b_1}-\phi_{a_1}\right)=\pi\end{cases}。\tag{11}$$

式(10)和式(11)可视为面内单向散射的Kerker条件。

4.2　矢量光场对等离激元远场辐射的调控

如前所述，通过聚焦矢量光场的调控，可以设计矢量焦场各电磁分量的大小与相位，以此满足Kerker条件，实现等离激元核壳结构面内单向散射的目的。以聚焦的角向矢量光为例，如图9(a)所示，其焦场电磁场分量的比值会随焦平面的位置发生变化。因而，可以通过移动纳米球的位置使电磁场分量比值匹配Mie散射系数a_1和b_1的比值，以满足面内单向散射的振幅条件。同时，由图9(b)可知，电磁场分量E_y和ZH_z之间存在$\pi/2$的相位差。通过选择激发光波长，可叠加纳米球共振的相位跃变[图9(c)]，进一步满足面内单向散射的相位条件。基于此，将内外半径分别为$R_{\mathrm{in}}=106$ nm和$R_{\mathrm{out}}=206$ nm的单个核壳置于距焦场中心

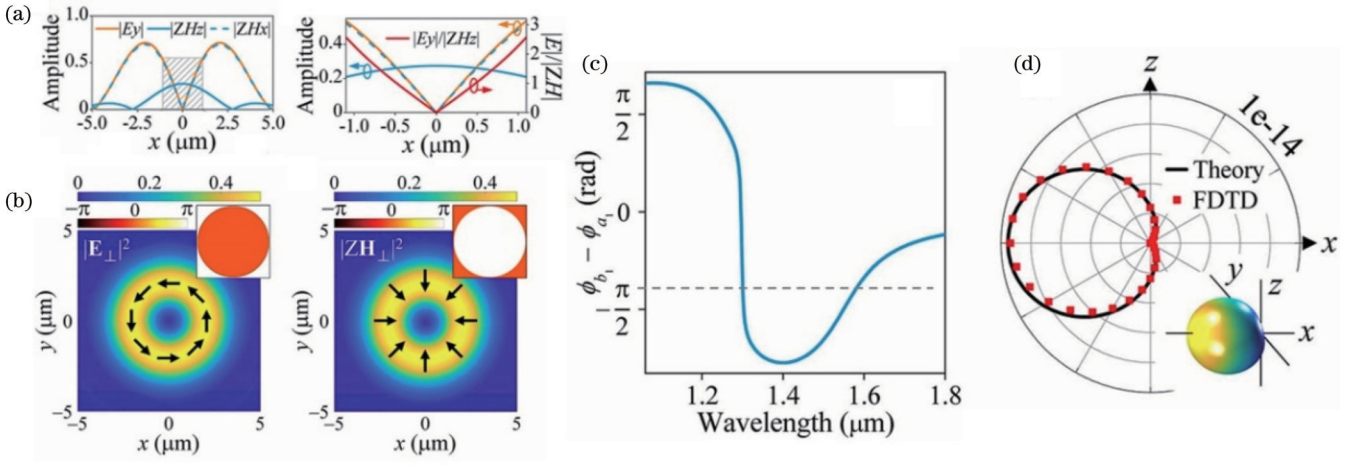

图9　紧聚焦角向矢量光对等离激元核壳纳米球的散射方向调控[70]。(a)角向矢量光束焦场的不同电磁场分量在x轴上的分布；(b)角向矢量光的横向电场($|E_\perp|^2=|E_x|^2+|E_y|^2$)和磁场强度($|ZH_\perp|^2=|ZH_x|^2+|ZH_y|^2$)的分布；(c)核壳纳米球Mie散射系数$a_1$和$b_1$的相位差的谱分布；(d)核壳纳米球在1550 nm波长处的远场单向散射分布

Fig. 9　Manipulating scattering pattern of plasmonic core-shell nanosphere with tightly focused azimuthally polarized vector beam[70]. (a) Distributions of electromagnetic components of azimuthally polarized vector beam along x direction of focal plane; (b) in-plane electric field ($|E_\perp|^2=|E_x|^2+|E_y|^2$) and magnetic field intensity ($|ZH_\perp|^2=|ZH_x|^2+|ZH_y|^2$) of azimuthally polarized vector beam; (c) spectrum distribution of phase difference between Mie coefficients a_1 and b_1 of core-shell nanospheres; (d) far-field unidirectional scattering distribution of core-shell nanosphrere at $\lambda=1550$ nm

x=73 nm处，并调节激发波长为1550 nm，可实现面内向左的远场单向散射[70]，如图9(d)所示。

利用矢量光场调控等离激元结构的辐射方向，为提升纳米光子器件的光波收集效率，研发高灵敏度的传感器件提供了新的解决方案。2014年，Neugebauer等[12]研究了紧聚焦径向矢量光激发下金纳米球的远场散射特性，如图10(a)所示。紧聚焦的矢量光可在金纳米球中激发出横向自旋偶极子和电偶激子。改变小球在焦场中的位置，他们观察到两类偶极子辐射电磁场的相长和相消干涉，以此实现了面内辐射场由各向同性到单向散射的转变[图10(b)]。进一步，他们将金纳米球集成于介质波导阵列中，借助纳米球的单向散射，实现了光场向介质波导的定向耦合[图10(c)]，展示了该混合结构在全光开关应用的可能。2020年，Zang等[71]提出了一种矢量光场调制的表面等离极化激元单向传播的方案，如图10(d)所示。他们利用聚焦的厄米高斯光，在光学纳米槽孔天线中激发了一对磁偶极模式[如图10(e)上图所示]。通过在聚焦场中移动槽孔天线，可改变其磁偶模式的相位差，以满足两模式的相长和相消干涉，以此实现向左或向右单向传输的表面等离极化激元[如图10(e)下图所示]。进一步，他们得到了表面等离极化激元传播方向与槽孔天

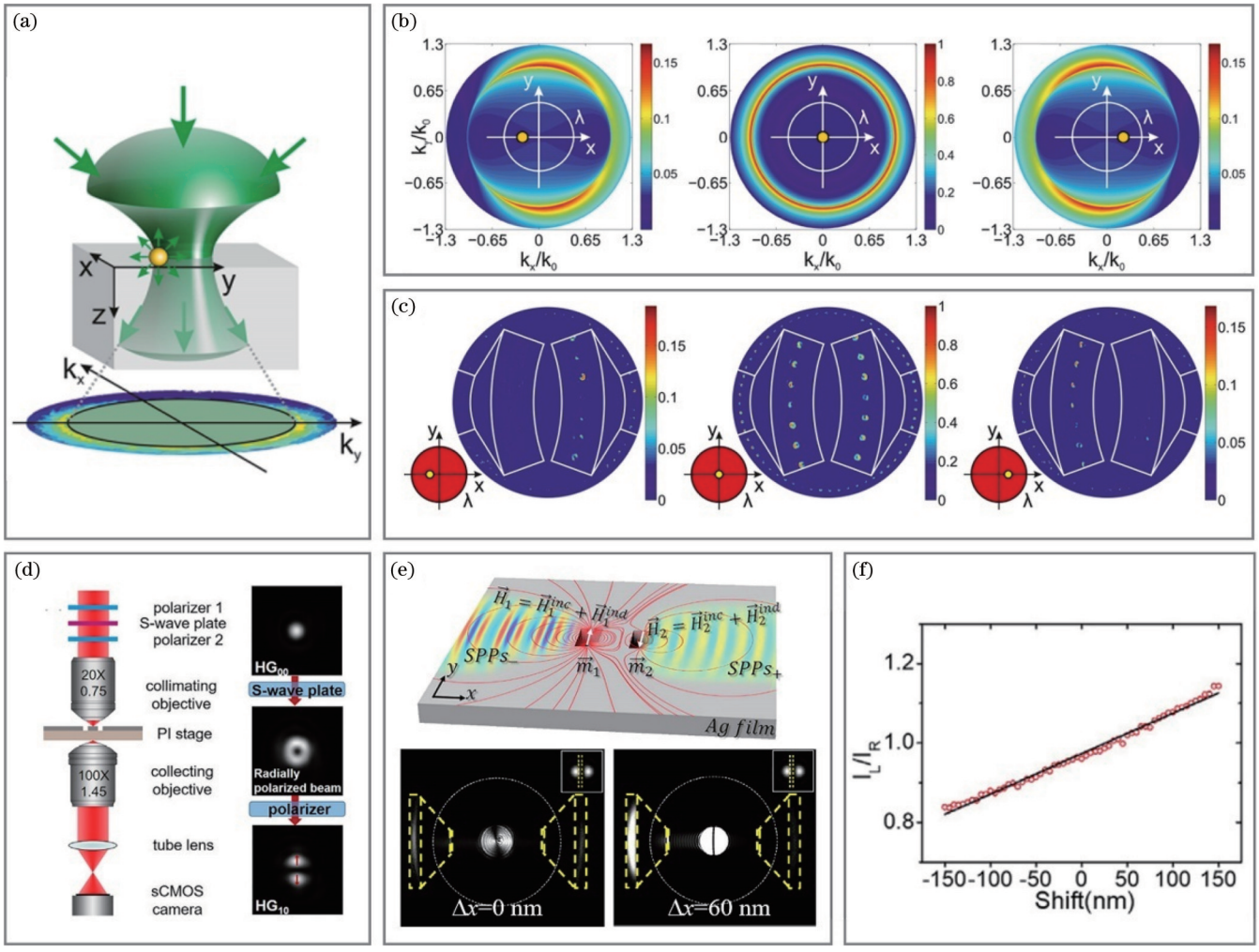

图10　矢量光场调控的金纳米结构的单向散射。(a) 利用紧聚焦矢量光操控的金纳米球远场散射的示意图[12]；(b) 金纳米球在焦场位置的变化可令面内辐射场由各向同性(中图)变为单向性散射(左、右图)[12]；(c) 金纳米球单向散射在波导定向耦合中的应用[12]；(d) 紧聚焦厄米-高斯光束激发槽孔天线表面等离激元的光路示意图[71]；(e) 槽孔天线中磁偶模式的激发(上图)与单向传输的表面等离极化激元(下图)[71]；(f) 非对称传输的表面等离极化激元在纳米位移传感中的应用[71]

Fig. 10　Unidirectional scattering of Au nanosctructure using vector beam control. (a) Schematic of far-field scattering of Au nanosphere controlled by tightly focused vector beam[12]; (b) change in focal field position of Au nanospheres can cause in-plane radiation field to shift from isotropic (center image) to unidirectional scattering (left and right images) [12]; (c) application of unidirectional scattering of Au nanospheres in waveguide directional coupling [12]; (d) optical path diagram of tightly focused Hermite-Gaussian beam exciting slotted antenna surface plasmon polariton[71]; (e) excitation of magnetic dipole modes in slot antennas (upper panel) and surface plasmon polaritons with unidirectional transmission (lower panel)[71]; (f) application of asymmetric transmission of surface plasmon polaritons in nanometric displacement sensing[71]

线的位置的依赖关系。据此规律，实现了亚纳米精度横向位移的测量，如图 10(f)所示。随后，他们将这一横向位移探测方法拓展到偏振编码的超表面系统中，使位移感测精度提升到 100 pm 量级，并结合移相方法将测量范围拓展到 200 μm 以上，消除了感测灵敏度的“死区”，使该传感器在高分辨光学成像、半导体加工、精密对准等应用方面迈出关键的一步[72]。

5 结 论

本文综述了近年来矢量光场与等离激元模式作用的进展。简要讨论了矢量光场匹配激发等离激元模式的本征响应理论。从等离激元杂化理论和耦合谐振子模型角度，解释了矢量光场对模式耦合的调控机理。通过 Mie 散射理论和 Kerker 条件，论述了矢量光场对等离激元远场辐射分布的调控方法。以此为基础，详细介绍了矢量光场在调控等离激元模式激发、耦合、辐射中的暗模式、Fano 共振和单向散射等过程中的新颖现象，以及在增强荧光和光学非线性、纳米尺度光操控、纳米位移传感等方面的应用。

需要指出的是，近十年来，基于矢量光场的等离激元模式调控得到了长足发展，但仍有许多问题亟待解决。典型地，由于衍射极限的存在，矢量光场与纳米尺度的等离激元结构存在较大的空间失配，导致偏振-偶极矩匹配的模式激发方法(特别是高阶模式)的效率较低。为此，需要发展极小尺度的聚焦场的产生方法，如借助镀金属膜的光纤探针生成纳米尺度的矢量光场[73]。再者，矢量光场等离激元模式耦合调控方面，多限于对称性较高的等离激元结构。如何在非对称金属结构中挑选并调控等离激元模式的耦合仍存在挑战。这需要发展更为精细、灵活的矢量光场的定制方法(如基于机器学习的光场调控技术[74])来准确调控等离激元模式。

值得注意的是，近年来光场调控研究得到了飞速发展，一些新型光场不断涌现，如高度局域手性“光针”[75]、具有拓扑特性的斯格明子[76]、光学莫比乌斯环[77]等。这些为人们利用光场调控技术操纵等离激元提供了巨大的机遇。与此同时，以等离激元纳米腔为代表的超紧凑等离激元结构逐渐兴起，成为实现极端局域光场的理想选择。可以预见的是，如将两者相结合，可赋予人们操控等离激元物性(如超手性场、局域光子态密度、模体积等)更为丰富的手段[78-79]，从而为纳米甚至皮米尺度下研究室温强耦合、光学非线性、手性光力学等基本物理现象提供更为便利的条件，并有望拓展等离激元在信息、能源、生物等领域的应用。

参 考 文 献

[1] Lal S, Link S, Halas N J. Nano-optics from sensing to waveguiding[J]. Nature Photonics, 2007, 1(11): 641-648.

[2] Kravets V G, Kabashin A V, Barnes W L, et al. Plasmonic surface lattice resonances: a review of properties and applications [J]. Chemical Reviews, 2018, 118(12): 5912-5951.

[3] Kawata S, Inouye Y, Verma P. Plasmonics for near-field nano-imaging and superlensing[J]. Nature Photonics, 2009, 3(7): 388-394.

[4] Atwater H A, Polman A. Plasmonics for improved photovoltaic devices[J]. Nature Materials, 2010, 9(3): 205-213.

[5] McFarland A D, Van Duyne R P. Single silver nanoparticles as real-time optical sensors with zeptomole sensitivity[J]. Nano Letters, 2003, 3(8): 1057-1062.

[6] Mubeen S, Lee J, Singh N, et al. An autonomous photosynthetic device in which all charge carriers derive from surface plasmons[J]. Nature Nanotechnology, 2013, 8(4): 247-251.

[7] Okamoto K, Niki I, Shvartser A, et al. Surface-plasmon-enhanced light emitters based on InGaN quantum wells[J]. Nature Materials, 2004, 3(9): 601-605.

[8] Zijlstra P, Chon J W M, Gu M. Five-dimensional optical recording mediated by surface plasmons in gold nanorods[J]. Nature, 2009, 459(7245): 410-413.

[9] Duan X Y, Kamin S, Liu N. Dynamic plasmonic colour display [J]. Nature Communications, 2017, 8: 14606.

[10] Zhang Y Q, Min C J, Dou X J, et al. Plasmonic tweezers: for nanoscale optical trapping and beyond[J]. Light: Science & Applications, 2021, 10: 59.

[11] Luk′yanchuk B, Zheludev N I, Maier S A, et al. The Fano resonance in plasmonic nanostructures and metamaterials[J]. Nature Materials, 2010, 9(9): 707-715.

[12] Neugebauer M, Bauer T, Banzer P, et al. Polarization tailored light driven directional optical nanobeacon[J]. Nano Letters, 2014, 14(5): 2546-2551.

[13] Feng F, Si G Y, Min C J, et al. On-chip plasmonic spin-Hall nanograting for simultaneously detecting phase and polarization singularities[J]. Light: Science & Applications, 2020, 9: 95.

[14] Yang A K, Li Z Y, Knudson M P, et al. Unidirectional lasing from template-stripped two-dimensional plasmonic crystals[J]. ACS Nano, 2015, 9(12): 11582-11588.

[15] Kim M, Lee J H, Nam J M. Plasmonic photothermal nanoparticles for biomedical applications[J]. Advanced Science, 2019, 6(17): 1900471.

[16] Sámson Z L, MacDonald K F, De Angelis F, et al. Metamaterial electro-optic switch of nanoscale thickness[J]. Applied Physics Letters, 2010, 96(14): 143105.

[17] Franklin D, Chen Y, Vazquez-Guardado A, et al. Polarization-independent actively tunable colour generation on imprinted plasmonic surfaces[J]. Nature Communications, 2015, 6: 7337.

[18] 潘岳, 丁剑平, 王慧田. 新型矢量光场调控: 简介、进展与应用[J]. 光学学报, 2019, 39(1): 0126001.
Pan Y, Ding J P, Wang H T. Manipulation on novel vector optical fields: introduction, advances and applications[J]. Acta Optica Sinica, 2019, 39(1): 0126001.

[19] 李润丰, 施可彬. 基于光场调控的高时空分辨率光学成像[J]. 光学学报, 2019, 39(1): 0126010.
Li R F, Shi K B. High spatiotemporal imaging based on optical field engineering[J]. Acta Optica Sinica, 2019, 39(1): 0126010.

[20] 罗嗣佐, 陈洲, 李孝开, 等. 超快飞秒激光场中原子分子量子态调控[J]. 光学学报, 2019, 39(1): 0126007.
Luo S Z, Chen Z, Li X K, et al. Controlling quantum states of atoms and molecules by ultrafast femtosecond laser fields[J]. Acta Optica Sinica, 2019, 39(1): 0126007.

[21] Cai Y J, Peschel U. Second-harmonic generation by an astigmatic partially coherent beam[J]. Optics Express, 2007, 15(23): 15480-15492.

[22] Cheng Z M, Xue S T, Lou Y C, et al. Rotational Doppler shift tripling via third-harmonic generation of spatially structured light in a quasi-periodically poled crystal[J]. Optica, 2023, 10(1): 20-25.

[23] Youngworth K S, Brown T G. Focusing of high numerical

aperture cylindrical-vector beams[J]. Optics Express, 2000, 7(2): 77-87.
[24] Markel V A. Antisymmetrical optical states[J]. Journal of the Optical Society of America B, 1995, 12(10): 1783-1791.
[25] Bergman D J, Stroud D. Theory of resonances in the electromagnetic scattering by macroscopic bodies[J]. Physical Review B, 1980, 22(8): 3527-3539.
[26] Fung K H, Kumar A, Fang N X. Electron-photon scattering mediated by localized plasmons: a quantitative analysis by eigen-response theory[J]. Physical Review B, 2014, 89(4): 045408.
[27] Fung K H, Chan C T. Plasmonic modes in periodic metal nanoparticle chains: a direct dynamic eigenmode analysis[J]. Optics Letters, 2007, 32(8): 973-975.
[28] Man Z S, Du L P, Min C J, et al. Dynamic plasmonic beam shaping by vector beams with arbitrary locally linear polarization states[J]. Applied Physics Letters, 2014, 105(1): 011110.
[29] Weng X Y, Du L P, Yang A P, et al. Generating arbitrary order cylindrical vector beams with inherent transform mechanism[J]. IEEE Photonics Journal, 2017, 9(1): 6100208.
[30] Sancho-Parramon J, Jelovina D. Boosting Fano resonances in single layered concentric core-shell particles[J]. Nanoscale, 2014, 6(22): 13555-13564.
[31] Panaro S, Nazir A, Liberale C, et al. Dark to bright mode conversion on dipolar nanoantennas: a symmetry-breaking approach[J]. ACS Photonics, 2014, 1(4): 310-314.
[32] Knight M W, Wu Y P, Lassiter J B, et al. Substrates matter: influence of an adjacent dielectric on an individual plasmonic nanoparticle[J]. Nano Letters, 2009, 9(5): 2188-2192.
[33] Krasavin A V, Segovia P, Dubrovka R, et al. Generalization of the optical theorem: experimental proof for radially polarized beams[J]. Light: Science & Applications, 2018, 7: 36.
[34] Bag A, Neugebauer M, Mick U, et al. Towards fully integrated photonic displacement sensors[J]. Nature Communications, 2020, 11: 2915.
[35] Xiao F J, Wang G L, Gan X T, et al. Selective excitation of a three-dimensionally oriented single plasmonic dipole[J]. Photonics Research, 2019, 7(6): 693-698.
[36] Scheuer J. Ultra-high enhancement of the field concentration in Split Ring Resonators by azimuthally polarized excitation[J]. Optics Express, 2011, 19(25): 25454-25464.
[37] Gómez D E, Teo Z Q, Altissimo M, et al. The dark side of plasmonics[J]. Nano Letters, 2013, 13(8): 3722-3728.
[38] Herzog J B, Knight M W, Li Y J, et al. Dark plasmons in hot spot generation and polarization in interelectrode nanoscale junctions[J]. Nano Letters, 2013, 13(3): 1359-1364.
[39] Celebrano M, Wu X F, Baselli M, et al. Mode matching in multiresonant plasmonic nanoantennas for enhanced second harmonic generation[J]. Nature Nanotechnology, 2015, 10(5): 412-417.
[40] Wu C, Khanikaev A B, Adato R, et al. Fano-resonant asymmetric metamaterials for ultrasensitive spectroscopy and identification of molecular monolayers[J]. Nature Materials, 2012, 11(1): 69-75.
[41] Hakala T K, Rekola H T, Väkeväinen A I, et al. Lasing in dark and bright modes of a finite-sized plasmonic lattice[J]. Nature Communications, 2017, 8: 13687.
[42] Schmidt F P, Ditlbacher H, Hohenester U, et al. Dark plasmonic breathing modes in silver nanodisks[J]. Nano Letters, 2012, 12(11): 5780-5783.
[43] Yang S C, Kobori H, He C L, et al. Plasmon hybridization in individual gold nanocrystal dimers: direct observation of bright and dark modes[J]. Nano Letters, 2010, 10(2): 632-637.
[44] Shang W Y, Xiao F J, Zhu W R, et al. Characterizing localized surface plasmon resonances using focused radially polarized beam [J]. Applied Optics, 2019, 58(21): 5812-5816.
[45] Yanai A, Grajower M, Lerman G M, et al. Near- and far-field properties of plasmonic oligomers under radially and azimuthally polarized light excitation[J]. ACS Nano, 2014, 8(5): 4969-4974.
[46] Bao Y J, Zhu X, Fang Z Y. Plasmonic toroidal dipolar response under radially polarized excitation[J]. Scientific Reports, 2015, 5: 11793.
[47] Anger P, Bharadwaj P, Novotny L. Enhancement and quenching of single-molecule fluorescence[J]. Physical Review Letters, 2006, 96(11): 113002.
[48] Zhang L, Meng C, Yang H, et al. Azimuthal vector beam illuminating plasmonic tips circular cluster for surface-enhanced Raman spectroscopy[J]. Chinese Optics Letters, 2023, 21(3): 033603.
[49] Xiao F J, Ren Y X, Shang W Y, et al. Sub-10 nm particle trapping enabled by a plasmonic dark mode[J]. Optics Letters, 2018, 43(14): 3413-3416.
[50] Zhang J C, Lu F F, Zhang W D, et al. Optical trapping of single nano-size particles using a plasmonic nanocavity[J]. Journal of Physics: Condensed Matter, 2020, 32(47): 475301.
[51] Xiao F J, Shang W Y, Zhu W R, et al. Cylindrical vector beam-excited frequency-tunable second harmonic generation in a plasmonic octamer[J]. Photonics Research, 2018, 6(3): 157-161.
[52] Prodan E, Radloff C, Halas N J, et al. A hybridization model for the plasmon response of complex nanostructures[J]. Science, 2003, 302(5644): 419-422.
[53] Prodan E, Nordlander P. Plasmon hybridization in spherical nanoparticles[J]. The Journal of Chemical Physics, 2004, 120(11): 5444-5454.
[54] Joe Y S, Satanin A M, Kim C S. Classical analogy of Fano resonances[J]. Physica Scripta, 2006, 74(2): 259-266.
[55] Deng T S, Parker J, Yifat Y, et al. Dark plasmon modes in symmetric gold nanoparticle dimers illuminated by focused cylindrical vector beams[J]. The Journal of Physical Chemistry C, 2018, 122(48): 27662-27672.
[56] Volpe G, Molina-Terriza G, Quidant R. Deterministic subwavelength control of light confinement in nanostructures[J]. Physical Review Letters, 2010, 105(21): 216802.
[57] Sancho-Parramon J, Bosch S. Dark modes and fano resonances in plasmonic clusters excited by cylindrical vector beams[J]. ACS Nano, 2012, 6(9): 8415-8423.
[58] Bao Y J, Hu Z J, Li Z W, et al. Magnetic plasmonic fano resonance at optical frequency[J]. Small, 2015, 11(18): 2177-2181.
[59] Xiao F J, Wang G L, Shang W Y, et al. Radial breathing modes coupling in plasmonic molecules[J]. Optics Express, 2019, 27(4): 5116-5124.
[60] Xiao F J, Zhang J C, Yu W X, et al. Reversible optical binding force in a plasmonic heterodimer under radially polarized beam illumination[J]. Optics Express, 2020, 28(3): 3000-3008.
[61] Xiao F J, Cao S Y, Shang W Y, et al. Enhanced second-harmonic generation assisted by breathing mode in a multi-resonant plasmonic trimer[J]. Optics Letters, 2019, 44(15): 3813-3816.
[62] Shang W Y, Xiao F J, Zhu W R, et al. Fano resonance with high local field enhancement under azimuthally polarized excitation[J]. Scientific Reports, 2017, 7: 1049.
[63] Fu Y H, Kuznetsov A I, Miroshnichenko A E, et al. Directional visible light scattering by silicon nanoparticles[J]. Nature Communications, 2013, 4: 1527.
[64] Kerker M, Wang D S, Giles C L. Electromagnetic scattering by magnetic spheres[J]. Journal of the Optical Society of America, 1983, 73(6): 765-767.
[65] Kosako T, Kadoya Y, Hofmann H F. Directional control of light by a nano-optical Yagi-Uda antenna[J]. Nature Photonics, 2010, 4(5): 312-315.
[66] Vercruysse D, Sonnefraud Y, Verellen N, et al. Unidirectional side scattering of light by a single-element nanoantenna[J]. Nano Letters, 2013, 13(8): 3843-3849.
[67] Shegai T, Chen S, Miljković V D, et al. A bimetallic

nanoantenna for directional colour routing[J]. Nature Communications, 2011, 2: 481.
[68] Shegai T, Johansson P, Langhammer C, et al. Directional scattering and hydrogen sensing by bimetallic Pd - Au nanoantennas[J]. Nano Letters, 2012, 12(5): 2464-2469.
[69] Wang M Y, Li M Q, Jiang S, et al. Plasmonics meets super-resolution microscopy in biology[J]. Micron, 2020, 137: 102916.
[70] Shang W Y, Xiao F J, Zhu W R, et al. Unidirectional scattering exploited transverse displacement sensor with tunable measuring range[J]. Optics Express, 2019, 27(4): 4944-4955.
[71] Zang T Y, Zang H F, Xi Z, et al. Asymmetric excitation of surface plasmon polaritons via paired slot antennas for angstrom displacement sensing[J]. Physical Review Letters, 2020, 124 (24): 243901.
[72] Zang H F, Xi Z, Zhang Z Y, et al. Ultrasensitive and long-range transverse displacement metrology with polarization-encoded metasurface[J]. Science Advances, 2022, 8(41): eadd1973.
[73] Lu F F, Zhang W D, Zhang L, et al. Nanofocusing of surface plasmon polaritons on metal-coated fiber tip under internal excitation of radial vector beam[J]. Plasmonics, 2019, 14(6): 1593-1599.
[74] Giordani T, Suprano A, Polino E, et al. Machine learning-based classification of vector vortex beams[J]. Physical Review Letters, 2020, 124(16): 160401.
[75] Hu H F, Gan Q Q, Zhan Q W. Generation of a nondiffracting superchiral optical needle for circular dichroism imaging of sparse subdiffraction objects[J]. Physical Review Letters, 2019, 122 (22): 223901.
[76] Du L P, Yang A P, Zayats A V, et al. Deep-subwavelength features of photonic skyrmions in a confined electromagnetic field with orbital angular momentum[J]. Nature Physics, 2019, 15(7): 650-654.
[77] Bauer T, Banzer P, Karimi E, et al. Observation of optical polarization Möbius strips[J]. Science, 2015, 347(6225): 964-966.
[78] Li G C, Lei D Y, Qiu M, et al. Light-induced symmetry breaking for enhancing second-harmonic generation from an ultrathin plasmonic nanocavity[J]. Nature Communications, 2021, 12: 4326.
[79] Vento V, Roelli P, Verlekar S, et al. Mode-specific coupling of nanoparticle-on-mirror cavities with cylindrical vector beams[J]. Nano Letters, 2023, 23(11): 4885-4892.

Plasmonic Mode Control Based on Vector Beams

Xiao Fajun[1,2*], Zhao Jianlin[1,2**]

[1]*School of Physical Science and Technology, Northwestern Polytechnical University, Xi'an* 710129, *Shaanxi, China*;

[2]*Key Laboratory of Light Field Regulation and Information Perception, Ministry of Industry and Information Technology, Northwestern Polytechnical University, Xi'an* 710129, *Shaanxi, China*

Abstract

Significance Owing to the remarkable field confinement ability, surface plasmons have become an ideal platform for investigating light-matter interactions at the sub-wavelength scale. The intriguing properties make surface plasmons the fundamental block for future optoelectronic applications, including biomedical detection, photocatalysis, nanolaser, and data storage. Notably, the aforementioned fundamental and application research calls for surface plasmons with large tunability. Conventionally, the properties of surface plasmons can be tailored by changing the size, shape, environmental refractive index, and gap of the structure. However, these methods are usually static and lack of flexibility.

Recently, the advance of light field manipulation has expanded the dimension of light utilization and provided rich and flexible strategies for regulating light-matter interactions. For example, through the amplitude, phase, and polarization modulation of the light field, a variety of super-resolution imaging techniques have been developed. Precise control of molecular rotation, dissociation, and ionization can be achieved by employing the time domain regulation of the light field. By controlling the coherence and polarization state of the light field, the conversion efficiency of nonlinear optical processes can be improved. Correspondingly, these methods for controlling the light-matter interactions have also been successively applied to surface plasmons, which open up a new way for exploring novel phenomena and developing related applications.

Progress The eigen-response theory is first introduced to describe the polarization matching method to selectively excite plasmonic modes. We show the typical work on the tuning of dipole moment orientation [Fig. 2(b)] and the excitation of plasmonic dark modes (Fig. 3) with the aid of vector beams. The plasmonic mode controlling enables the generation of a strong local field to precisely manipulate the light-matter interactions at the single molecular level [Fig. 4(a)] and enhance the efficiency of surface-enhanced Raman spectroscopy [Fig. 4(b)]. Additionally, the nanosize particles with ultrasmall hot spots are trapped [Figs. 4(c) and 4(d)], and the optical upconversion frequency of a plasmonic octamer is tuned [Fig. 4(e)].

Subsequently, the mechanism for controlling plasmonic mode coupling is explained in the frameworks of plasmon hybrid theory (Fig. 5) and coupled harmonic oscillator model (Fig. 6). Specifically, we present the work on controlling the bonding and antibonding modes of the plasmonic dimer with vector beams [Fig. 7(a)]. In 2010, Volpe *et al*. demonstrated

a method to deterministically control the local field of the plasmonic nanostructure. They employed the optical inversion algorithm to superpose the Hermit-Gaussian beams with different amplitudes and phases to construct the vector excitation and successfully produce the target local field distribution as shown in Fig. 7(b). Meanwhile, we emphasize the excitation progress of single and multiple Fano resonances in highly symmetric plasmonic nanoclusters using the vector beams [Figs. 7(c) and 7(d)]. In addition, we show the applications of controlling plasmonic mode coupling in the optical binding force reversion [Fig. 8(a)], enhanced second harmonic generation [Fig. 8(b)], and the detection of structural defect and beam misalignment [Fig. 8(c)].

Finally, the method to control the far-field scattering of plasmonic structures with vector beams is interpreted by combing Mie theory and Kerker condition. As an example, we show that the unidirectional scattering of a core-shell plasmonic nanosphere can be achieved by adjusting the phase differences and amplitude between electric and magnetic dipoles (Fig. 9). Interestingly, the tightly focused radially polarized beams can excite a spinning dipole moment in an Au nanosphere [Fig. 10(a)]. The polarization distribution at the focal plane allows for tuning the emission from a homogeneous to a unidirectional pattern by simply moving the particle relative to the beam axis [Fig. 10(b)], which is found to have an application in the directional coupling to a planar two-dimensional dielectric waveguide [Fig. 10(c)]. Additionally, Zang *et al*. demonstrate a method to realize the asymmetric excitation of surface plasmon polaritons (SPPs) by illuminating a pair of slot antennas with the Hermite-Gaussian beam [Fig. 10(e)]. They summarized the asymmetric intensity ratio of the SPP pattern as a displacement function of slot antennas [Fig. 10(f)], delayering a displacement sensor with angstrom precision.

Conclusions and Prospects We briefly introduce the basic theory and physical mechanism of the interactions between vector beams and plasmonic modes and review the recent progress of plasmon mode excitation, coupling, and far-field radiation regulated by the vector beams. Furthermore, their applications in enhanced spectroscopy, nanometric optical trapping, and nano-displacement sensing are introduced. It is worth noting that the research on light field manipulation is still in a rapid development track, and some new types of light fields have been emerging, such as the superchiral optical needle, photonic skyrmions with topological features, and optical Möbius strips. These advances provide great opportunities for people to control plasmonic modes with extra freedom. Meanwhile, ultra-compact plasmonic structures represented by plasmonic nanocavities have emerged as a promising route to squeeze light into the true nanoscale level. It is foreseeable that if the merits of these two aspects are combined, one will have more abundant strategies to manipulate the optical properties of surface plasmons, ranging from the mode volume and optical chirality to the local optical density of the state. In this sense, it would open up a new avenue for studying basic physical phenomena such as strong coupling at room temperature, optical nonlinearity, and polarization-dependent optomechanics. Then, it will undoubtedly expand the applications of surface plasmons in information, energy, biology, and many other fields.

Key words surface plasmons; vector beams; mode coupling; unidirectional scattering